DOI: 10.1002/ejic.200801254

Chirality in the Photochemical *mer*→*fac* Geometrical Isomerization of Tris(1-phenylpyrazolato,*N*,$C^{2'}$)iridium(III)

Kazuyoshi Tsuchiya,[a] Etsuko Ito,[a] Shiki Yagai,[a] Akihide Kitamura,[a] and Takashi Karatsu*[a]

Keywords: Iridium / Isomerization / Chirality / Photochemistry

Irradiation of the optically resolved *mer*-Δ isomer of tris(1-phenylpyrazolato,*N*,$C^{2'}$)iridium(III) with 366-nm light in CH_3CN purged by argon at 25 °C gave 59 % *fac*-Δ and 41 % *fac*-Λ (18 % *ee*) at the end of geometrical isomerization. Formation of the intermediate *mer*-Λ species was not observed, which is quite characteristic when compared with the corresponding thermal isomerization reaction. This enantiomeric photoisomerization is rationally explained by a mechanism based on Ir–N bond dissociation at the top or bottom axial ligand. This reaction mechanism is explained by the potential energy surface of the triplet excited state.

(© Wiley-VCH Verlag GmbH & Co. KGaA, 69451 Weinheim, Germany, 2009)

Introduction

Iridium triscyclometalated complexes have recently attracted significant attention because of their supreme phosphorescence performance for OLEDs (organic light-emitting diodes).[1–5] For those materials, understanding of the behavior of the excited states including radiative and nonradiative processes are very important to prepare complexes with high emission efficiency and stability.

Triscyclometalated complexes such as tris(2-phenylpyridinato,*N*,$C^{2'}$)iridium(III) [Ir(ppy)$_3$] have meridional (*mer*) and facial (*fac*) geometrical isomers. The *fac* isomer is the thermodynamically controlled product in their synthesis and is generally strongly phosphorescent, whereas the corresponding *mer* isomer is the kinetically controlled product and weakly phosphorescent in solution at ambient temperature. Although several reports on the preparation of *mer* isomers have recently appeared for iridium complexes, their photochemical properties remains unclear.[6,7] Among them, we are interested in tris(1-phenylpyrazolato,*N*,$C^{2'}$)-iridium(III) [Ir(ppz)$_3$, Scheme 1], as both the *mer* and *fac* isomers give no phosphorescence in solution at ambient temperature.[6,7] The main reason for this was reported to be the location of the thermally equilibrated nonradiative excited state just above the emissive state,[8,9] and the absence of phosphorescence from the *mer* isomer is partly due to the *mer*→*fac* geometrical isomerization.[6,7] Ir(ppz)$_3$ is reasonably phosphorescent in the solid phase, and therefore, a blue-emitting OLED device has been fabricated.[10] In addition, Ir(ppz)$_3$ is not only used as a part of a dopant to give white emission,[11] but it is also used as a material for electron blocking layer.[12]

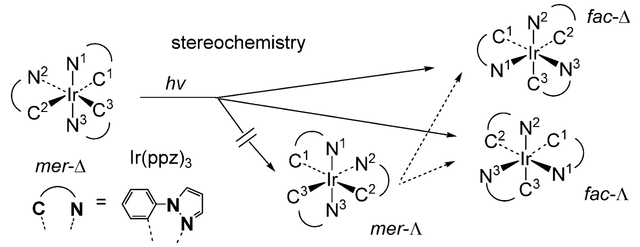

Scheme 1. Enantiomers and geometrical isomers in the photochemical isomerization of Ir(ppz)$_3$.

In this work we addressed how the chirality of the *mer* isomer is transferred to the *fac* isomer in the photochemical *mer*→*fac* geometrical isomerization of Ir(ppz)$_3$. Interestingly, we found that the intermediate *mer*-Λ is not generated upon irradiation of *mer*-Δ. This cannot be explained by faster *mer*→*fac* isomerization than *mer*-Δ→*mer*-Λ isomerization, that is, the two processes are not parallel. The isomerization seems to proceed through a ligand dissociation–association mechanism, and as a result, the geometrical isomerization must accompany the optical isomerization. Once *mer*-Λ is produced by the irradiation of *mer*-Δ, both isomers behave similarly. Thus, selective disappearance of only *mer*-Λ does not occur. We propose a plausible mechanism based on DFT calculations.

Results and Discussion

Ir(ppz)$_3$ was synthesized according to the method reported previously.[8] The *mer* and the *fac* isomers were sepa-

---

[a] Department of Applied Chemistry and Biotechnology, Graduate School of Engineering, Chiba University,
1-33 Yayoi-cho, Inage-ku, Chiba 263-8522, Japan
Fax: +81-43-290-3401
E-mail: karatsu@faculty.chiba-u.jp

rated by using conventional column chromatography, and both isomers were optically resolved to their Λ and Δ isomers (isomeric purity >98%) by using semipreparative chiral HPLC. Here, optical isomers having shorter and longer retention times in the HPLC can be determined as the Δ and Λ isomers, respectively, by comparing their circular dichroism (CD) spectra with those reported for the optically resolved diastereomeric Ir(ppy)$_3$ derivatives, the chiralities of which were determined by X-ray crystallography.[13–16] The CD spectra of the *mer*-Δ, *mer*-Λ, *fac*-Δ, and *fac*-Λ isomers in CH_3CN are shown in Figure 1. The CD spectra of the enantiomers showed good mirror images of each other for both the *mer* and *fac* isomers.

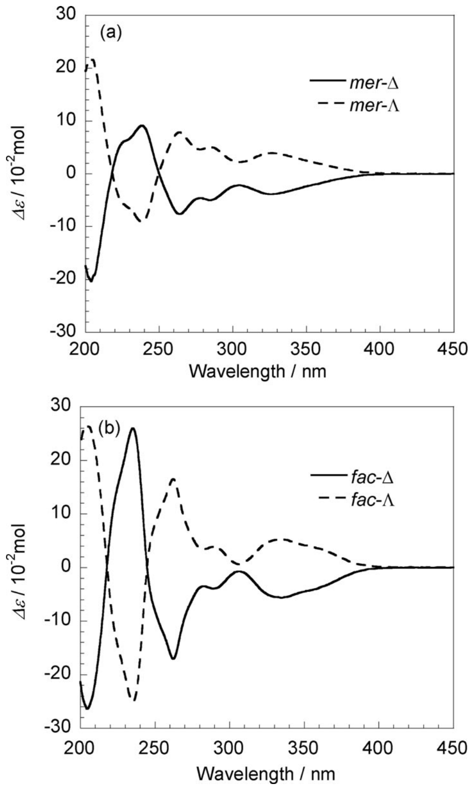

Figure 1. CD spectra of enantiomers of (a) *mer*-Ir(ppz)$_3$ and (b) *fac*-Ir(ppz)$_3$ in CH_3CN.

Each isomer (*mer*-Δ, *mer*-Λ, *fac*-Δ, and *fac*-Λ) was irradiated in CH_3CN purged by argon by using a 1 cm × 1 cm quartz cuvette by a 366-nm mercury lamp. The isomerization can be followed by HPLC, UV/Vis absorption (Figure 2c), or CD spectroscopy (Figure 2a,b). The enantiomer excess (*ee*) values were determined by both chiral HPLC and CD spectroscopy, and those values essentially matched within experimental errors.

Surprisingly, the irradiation of the *mer*-Δ isomer gave 59% *fac*-Δ and 41% *fac*-Λ (18%*ee*) at 25 °C at the end of geometrical isomerization. When isomerization is followed by CD spectra, the CD signal decreases in its intensity as shown in Figure 2a, and it does not completely disappear even at the end point of the geometrical isomerization achieved by the 45 s irradiation. Surprisingly, no formation of the *mer*-Λ isomers was observed during the geometrical isomerization (Figure 3). To our further surprise, enantioselectivity increased with temperature. Both of the *ee* and $\Phi_{mer\rightarrow fac}$ values increased as follows: 14%*ee*, Φ = 0.065 at –35 °C, 18%*ee*, Φ = 0.072 at 25 °C, and 23%*ee*, Φ = 0.073 at 70 °C. This phenomenon occurred similarly for the other enantiomer, that is, the irradiation of *mer*-Λ gave 18%*ee* of *fac*-Λ. Then, prolonged irradiation of the enantiomerically enriched solution of the *fac* isomers for 700 s gave complete racemization at all temperatures examined.

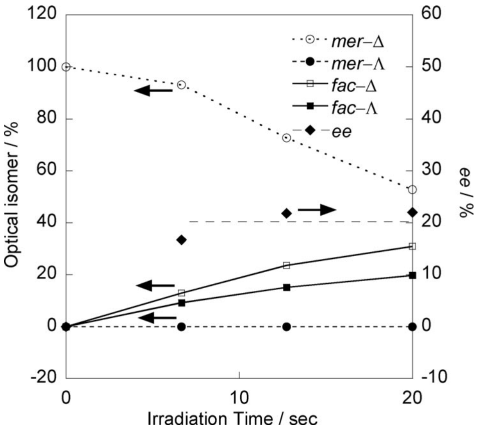

Figure 3. Conversion and formation of the optical isomers by irradiation and their enantiomer excess values.

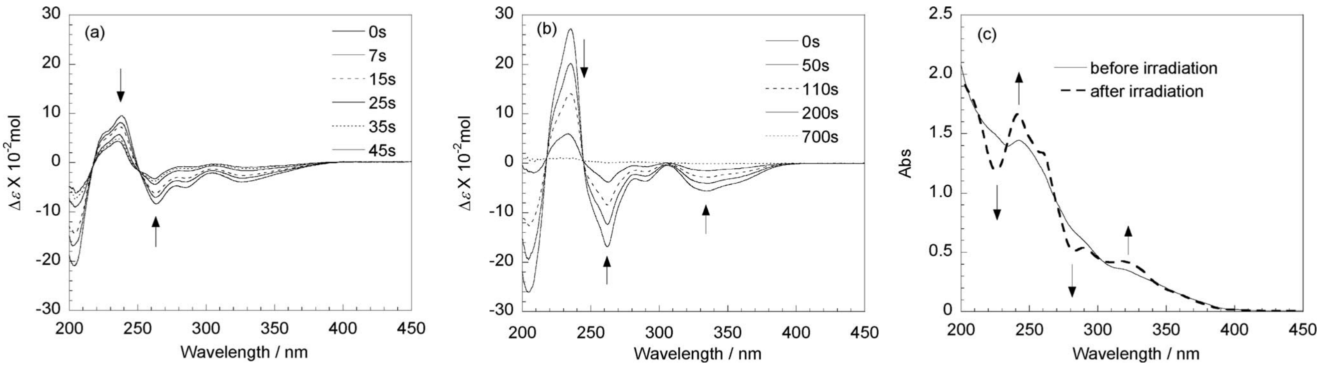

Figure 2. (a) CD spectral changes of the enantiomers of *mer*-Δ and (b) *fac*-Δ during photoirradiation at 366 nm; (c) UV absorption spectral change before and after irradiation of *mer*-Δ.

© 2009 Wiley-VCH Verlag GmbH & Co. KGaA, Weinheim

For the understanding of the photochemistry of the transition-metal complexes including triscyclometalated complexes, Adamson's empirical rule[17] and VC (Vanquickienborne–Ceulemans) theory[18] have been widely applied. The VC theory quantum chemically extends the selection rule by using the angular overlap model,[18c,18d] which includes not only σ-bond interaction but also π-bond interaction between the central Ir metal and the ligands. Photochemical substitution reactions of octahedral complexes obeys two rules: (i) The leaving ligand is located on the axis characterized by the weakest ligand field (LF). (ii) The leaving ligand on the labilized axis is the one exhibiting the strongest LF. In the case of *mer*-Ir(ppz)$_3$, there are three axes, and each axis has a pair of terminal coordination of (N,N), (N,C), and (C,C) to the central iridium atom. Therefore, the weakest LF combination is the N–Ir–N axis, which is photoactive. For this axis, both N–Ir bonds are the same, and thereby, the second rule is negligible.

We recently reported the properties of a series of iridium triscyclometalated complexes composed of 4-toluylpyridine (tpy) and 1-phenylpyrazole (ppz) ligands.[7b] The values of $\Phi_{mer\rightarrow fac}$ depend on the kind of axial ligands. Complexes possessing two ppz ligands such as Ir(ppz)$_3$ and Ir(ppz)$_2$(tpy) have higher $\Phi_{mer\rightarrow fac}$ (0.12 and 0.072, respectively) values than Ir(tpy)$_3$ and Ir(tpy)$_2$(ppz) complexes (1.8×10^{-4} and 2.3×10^{-4}, respectively). These results indicate that the bond dissociation occurs at the axial ligand, which matches the above rule, and the reason is not simply that the ppz ligand is much more labile than the ppy ligand.

In a separate experiment, the irradiation of *fac*-Δ did not produce *mer* isomers but instead produced *fac*-Λ with a quantum yield of 0.004 (this is ca. 1/18 of that of the geometrical isomerization). This photochemical reaction induced complete racemization (equal amounts of the enantiomers).

If the reaction starts from the *fac*-Δ isomer, the CD signal disappears completely after irradiation for 700 s (Figure 2b). This reaction may proceed through the Bailer twist mechanism as proposed for Ru complexes, because the racemization quantum yields are of the same order.[19] This inefficient twisting is not the main deactivation process of excitation energy. Nonradiative deactivation via a thermally accessible dd state might be an important route.[20]

We also tried to rationalize the mechanism of the present isomerization. Route A and B in Figure 4 proceed by Ir–N^1 and Ir–N^3 bond dissociations of the axial ligands, respectively, and these reactions proceed through rehybridization from square pyramidal (SP) to trigonal bipyramidal (TB) intermediates.[18] On the basis of statistical treatment of this mechanism, *mer*-Δ gives 5:8 of the *mer*-Δ returning and 1:8 of each *mer*-Λ, *fac*-Δ, and *fac*-Λ isomer formation. This product distribution partly fits the experimental result of the thermal isomerization described later, but does not fit the photochemical isomerization data described above. To rationalize our experimental results, we propose a possible mechanism. The reaction proceeds through the A1 or B1 route (rectangles in Figure 4). An important point is that the dissociation of the two axial bonds, Ir–N^1 or Ir–N^3, results in the formation of different enantiomers of *fac*-Ir(ppz)$_3$. Route A2 is difficult because this gives the *mer*-Λ isomer, which was not experimentally observed. The difference between routes A1/B1 and A2/B2 is how the axial axis is chosen in a TB structure. TB in routes A1/B1 or A2/B2 has N–Ir–C or C–Ir–C axes, respectively. However, there

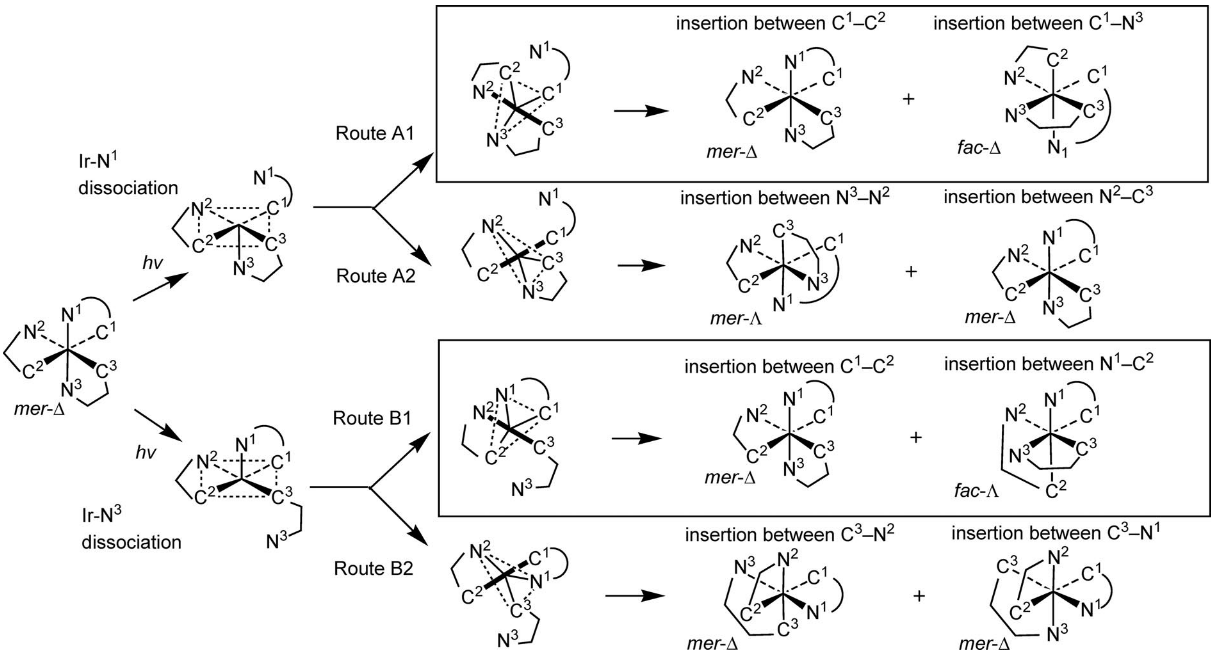

Figure 4. Plausible isomerization mechanism of chiral memorization in the geometrical isomerization of *mer*-Ir(ppz)$_3$ through trigonal bipyramidal intermediates. Central Ir atoms are omitted for clarity. See text for detailed explanations.

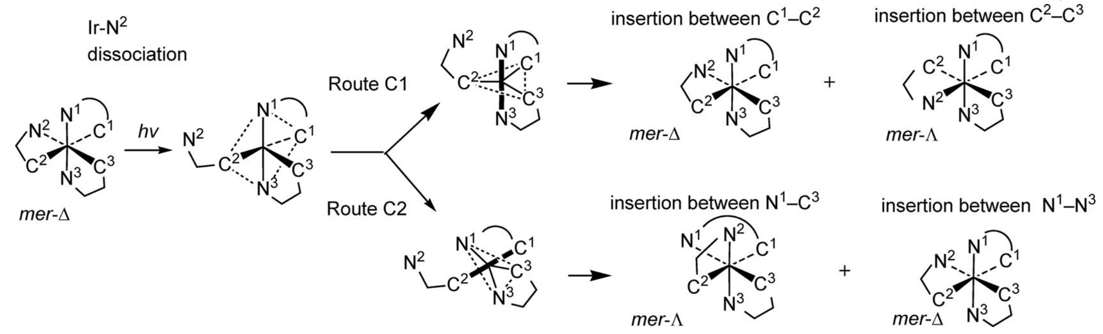

Figure 5. If the isomerization occurs through Ir–N^2 bond dissociation (equatorial ligand), it does not lead to geometrical isomerization.

are no rational reasons why A2 and B2 cannot occur. Therefore, the mechanism was modified so that the A2 and B2 routes proceed through rehybridization from the TB to SP intermediates. The C–Ir–C axis in TB is difficult to retain because of the strong *trans* effect. The TB intermediate rehybridizes to SP; recoordination of the N^1 or N^3 atom in the SP intermediate gives the *fac* isomer. The conversion from the C–Ir–C to C–Ir–N axis leads only to geometrical isomerization to form the *fac* isomer.

Moreover, Ir–N^2 bond dissociation (equatorial ligand) does not lead to geometrical isomerization (Figure 5). Participation of solvent molecules after dissociation is expected, as proposed for the thermal isomerization.[21] Examination of solvent effects is underway.

This isomerization was examined under thermochemical conditions. In refluxing dichlorobenzene at 180 °C for 8 h, chiral HPLC analyses indicated that 69% *mer*-Δ disappeared as a result of 55% ligand (ppz) dissociation from the complex; the formation of 9% *mer*-Λ, 1.6% *fac*-Δ, and 2.4% *fac*-Λ was also observed. Side products were formed; however, their quantitative analyses were difficult because of their low solubility. In any case, optical isomerization of the *mer* isomer occurred under thermal conditions, and this is in contrast to the results by photochemical isomerization.

Finally, this plausible isomerization mechanism is rationalized by quantum chemical calculations (Figure 6). A UB3LYP/LANL2DZ calculation indicates that HSOMO (highest singly occupied MO) α-spin-122 and vacant MOs α-123, 124 energies are close. Bond elongation of one of the axial Ir–N bonds from the optimized structure leads to potential energy surface crossing to dissociative dd states. These HSOMO must have antibonding interactions between the Ir and axial N atoms, which is similar to the recent study of a decay process involving the tridentate ligand of an Ir complex.[20] The α-122 HSOMO orbital has metal-to-ligand charge-transfer character for the fully optimized structure as shown in Figure 6 (left-hand side), and the structure has Ir–N^1 and Ir–N^3 bond lengths of 2.05 and 2.04 Å, respectively, which match the values obtained by X-ray single-crystal analysis (Ir–N^1 2.205 and Ir–N^3 2.013 Å).[6] In this structure, the lowest MO having an antibonding Ir–N bond is observed at α-132, and this is far above the HSOMO. However, optimized structures having elongated Ir–N^1 or Ir–N^3 bond lengths fixed at 2.80 Å have antibonding α-122 HSOMOs. In these structures, the Ir–N^2 and Ir–N^3 bond lengths were 2.14 and 2.27 Å for the former and the Ir–N^1 and Ir–N^2 bond lengths were 2.46 and 2.15 Å for the latter structure, respectively. Energy surface crossing as shown in

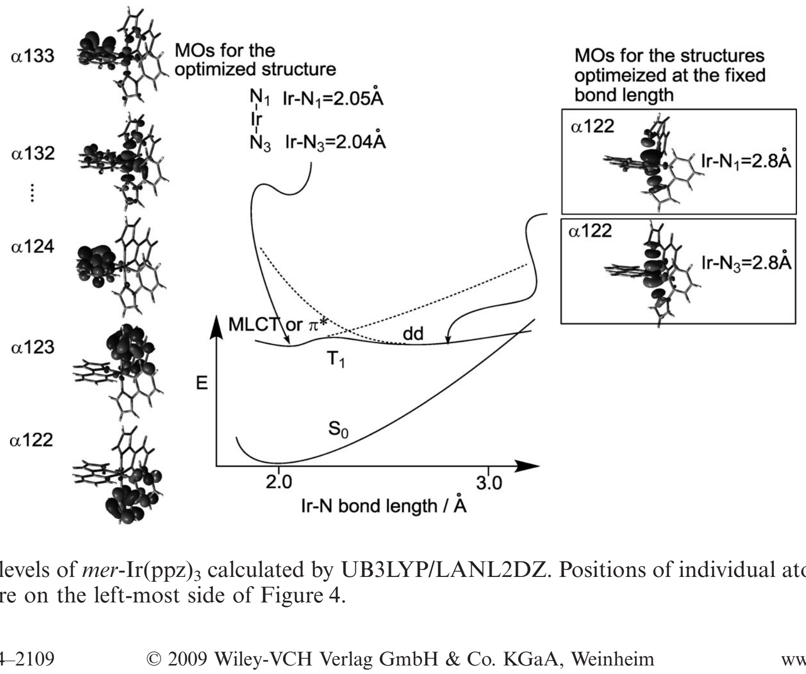

Figure 6. MOs and energy levels of *mer*-Ir(ppz)$_3$ calculated by UB3LYP/LANL2DZ. Positions of individual atoms in the structures match those shown in the structure on the left-most side of Figure 4.

Figure 6 leads to bond dissociation of the Ir–N^1 or Ir–N^3 bond, and this produces Λ-*fac* and Δ-*fac* isomers, respectively, as shown in Figure 4.

The shape of the potential energy surface controls the direction of bond elongation (Ir–N^1 or Ir–N^3) and finally the *ee* values. Calculated potential energies for bond-elongated structures were 2.8 kcal mol^{-1} higher (Ir–N^1 2.80 Å) and 0.5 kcal mol^{-1} lower (Ir–N^3 2.80 Å) than the energy of the fully optimized structure. These single-point energy calculation results do not fit the results of the *ee* values, because it is preferable to proceed to the B route to give the *fac*-Δ isomer. More calculations for the whole potential energy surface are necessary to obtain, for example, activation energies in the reaction coordinate. Those detailed calculations, including TD-DFT calculations, are ongoing in our group.

Conclusions

In conclusion, Δ–Λ optical isomerization accompanied in photochemical *mer–fac* geometrical isomerization was investigated for optically resolved Ir(ppz)$_3$ in solution. Irradiation of the optically resolved *mer*-Δ isomer with 366-nm light in CH$_3$CN purged with argon at 25 °C gave 59:41 *fac*-Δ/*fac*-Λ (18 %*ee*) at the end of geometrical isomerization. The lack of formation of the intermediate *mer*-Λ species is quite characteristic in comparison to the corresponding thermal isomerization process. This photoisomerization is rationally explained by a mechanism based on axial Ir–N^1 or Ir–N^3 bond dissociation–rehybridization–recoordination. Some DFT/UB3LYP calculation results of the triplet excited state rationally explain the selectivity of this isomerization.

Experimental Section

***fac*-Ir(ppz)$_3$:**[7b] ^{1}H NMR (396 MHz, CDCl$_3$): δ = 7.97 (d, J = 2.7 Hz, 3 H), 7.19 (dd, J = 7.8, 1.1 Hz, 3 H), 6.978 (d, J = 2.1 Hz, 3 H), 6.914 (ddd, J = 7.8, 7.1, 1.6 Hz, 3 H), 6.843 (dd, J = 7.5, 1.5 Hz, 3 H), 6.776 (ddd, J = 7.4, 7.2, 1.2 Hz, 3 H), 6.376 (dd, J = 2.4, 2.4 Hz, 3 H) ppm. ^{13}C NMR (99.45 MHz, CDCl$_3$): δ = 144.2, 139.8, 137.5, 136.7, 125.8, 124.9, 120.4, 110.8, 106.7 ppm. MS (FAB): *m*/*z* = 622.00.

***mer*-Ir(ppz)$_3$:**[7b] ^{1}H NMR (396 MHz, CDCl$_3$): δ = 8.00 (dd, J = 2.4, 0.5 Hz, 1 H), 7.95 (dd, J = 2.9, 0.7 Hz, 1 H), 7.91 (dd, J = 2.6, 0.7 Hz, 1 H), 7.281 (dd, J = 7.7, 0.8 Hz, 1 H), 7.24 (dd, J = 10.0, 0.8 Hz, 1 H), 7.19 (dd, J = 13.7,0.8 Hz, 1 H), 7.15 (d, J = 1.2 Hz, 1 H), 7.05 (dd, J = 7.1, 1.5 Hz, 1 H), 6.99–6.85 (m, 6 H) 6.81–6.75 (m, 3 H), 6.49 (dd, J = 7.5, 1.4 Hz, 1 H), 6.35–6.34 (m, 2 H), 6.30 (dd, J = 2.8, 2.2 Hz, 1 H) ppm. ^{13}C NMR (99.45 MHz, CDCl$_3$): δ = 152.3, 151.4, 145.9, 144.6, 142.9, 140.1, 139.9, 139.3, 139.0, 135.8, 135.2, 132.6, 126.3, 126.3, 126.0, 125.9, 124.8, 122.4, 121.9, 120.0, 111.5, 110.9, 110.9, 107.3, 107.3, 107.0 ppm. MS (FAB): *m*/*z* = 621.89.

DFT calculations were performed with the Gaussian 03 program by using the B3LYP/LANL2DZ or UB3LYP/LANL2DZ method.[22]

Acknowledgments

The authors thank Prof. Hugh D. Burrows (University of Coinbra) and Prof. Henrik Ottosson (Uppsala University) for their discussions. This work was supported by Grants-in-Aids for Scientific Research from the Ministry of Education, Culture, Sports, Science and Technology (MEXT) (No. 20550056).

---

[1] a) M. A. Baldo, D. F. O'Brien, Y. You, A. Shoustikov, S. Sibley, M. E. Thompson, S. R. Forrest, *Nature* **1998**, *395*, 151–154; b) M. A. Baldo, S. Lamansky, P. E. Burrows, M. E. Thompson, S. R. Forrest, *Appl. Phys. Lett.* **1999**, *75*, 4–6.

[2] H. Yersin (Ed.), *Highly Efficient OLEDs with Phosphorescent Materials*, Wiley-VCH, Weinheim, **2008** references cited therein.

[3] Y.-L. Tung, S.-W. Lee, Y. Chi, Y.-T. Tao, C.-H. Chien, Y.-M. Cheng, P.-T. Chou, S.-M. Peng, C.-S. Liu, *J. Mater. Chem.* **2005**, *15*, 460–464.

[4] A. Tsuboyama, H. Iwawaki, M. Furugori, T. Mukaide, J. Kamatani, S. Igawa, T. Moriyama, S. Miura, T. Takiguchi, S. Okada, M. Hoshino, K. Ueno, *J. Am. Chem. Soc.* **2003**, *125*, 12971–12979.

[5] S. Tokito, T. Iijima, T. Tsuzuki, F. Sato, *Appl. Phys. Lett.* **2003**, *83*, 2459–2461.

[6] A. Tamayo, B. D. Alleyne, P. I. Djurovich, S. Lamansky, I. Tsyba, N. N. Ho, R. Bau, M. E. Thompson, *J. Am. Chem. Soc.* **2003**, *125*, 7377–7387.

[7] a) T. Karatsu, T. Nakamura, S. Yagai, A. Kitamura, M. Matsushima, Y. Hori, T. Hagiwara, *Chem. Lett.* **2003**, *32*, 886–887; b) T. Karatsu, E. Itoh, S. Yagai, A. Kitamura, *Chem. Phys. Lett.* **2006**, *424*, 353–357.

[8] a) T. Sajoto, P. I. Djurovich, A. Tamayo, M. Yousufuddin, R. Bau, M. E. Thompson, R. J. Holmes, S. R. Forrest, *Inorg. Chem.* **2005**, *44*, 7992–8003; b) A. B. Tamayo, S. Garon, T. Sajoto, P. I. Djurovich, I. M. Tsyba, R. Bau, M. E. Thompson, *Inorg. Chem.* **2005**, *44*, 8723–8732.

[9] G. Choi, J. Lee, N. Park, Y. Kim, *Mol. Cryst. Liq. Cryst.* **2004**, *424*,173–185.

[10] E. J. Nam, J. H. Kim, B.-O. Kim, S. M. Kim, N. G. Park, Y. S. Kim, Y. K. Kim, Y. Y. Ha, *Bull. Chem. Soc. Jpn.* **2004**, *77*, 751–755.

[11] a) H. Kanno, R. J. Holmes, Y. Sun, S. Kena-Cohen, S. R. Forrest, *Adv. Mater.* **2006**, *18*, 339–342; b) E. L. Williams, K. Haavisto, J. Li, G. E. Jabbour, *Adv. Mater.* **2007**, *19*, 197–202; c) Y. Sun, S. R. Forrest, *Appl. Phys. Lett.* **2007**, *91*, 263503–06.

[12] a) V. I. Adamovich, S. R. Cordero, P. I. Djurovich, A. Tamayo, M. E. Thompson, B. W. D'Andrade, S. R. Forrest, *Org. Electron.* **2003**, *4*, 77–87; b) R. J. Holmes, S. R. Forresta, T. Sajoto, A. Tamayo, P. I. Djurovich, M. E. Thompson, J. Brooks, Y.-J. Tung, B. W. D'Andrade, M. S. Weaver, R. C. Kwong, J. J. Brown, *Appl. Phys. Lett.* **2005**, *87*, 243507–09; c) B. W. D'Andrade, S. Datta, S. R. Forrest, P. Djurovich, E. Polikarpov, M. E. Thompson, *Org. Electron.* **2005**, *6*, 11–20.

[13] C. Schaffner-Hamann, A. von Zelewsky, A. Barbieri, F. Barigelletti, G. Muller, J. P. Riehl, A. Neels, *J. Am. Chem. Soc.* **2004**, *126*, 9339–9348.

[14] F. J. Coughlin, M. S. Westrol, K. D. Oyler, N. Byrne, C. Kraml, E. Zysman-Colman, M. S. Lowry, S. Bernhard, *Inorg. Chem.* **2008**, *47*, 2039–2048.

[15] a) X. Chen, Y. Okamoto, T. Yano, J. Otsuki, *J. Sep. Sci.* **2007**, *30*, 713–716; b) J. Otsuki, T. Tokimoto, Y. Noda, T. Yano, T. Hasegawa, X. Chen, Y. Okamoto, *Chem. Eur. J.* **2007**, *13*, 2311–2319.

[16] A. Auffrant, A. Barbieri, F. Barigelletti, J. Lacour, P. Mobian, J.-P. Collin, J.-P. Sauvage, B. Ventura, *Inorg. Chem.* **2007**, *46*, 6911–6919.

[17] A. W. Adamson, *J. Phys. Chem.* **1967**, *71*, 798–808.

[18] a) L. G. Vanquickienborne, A. Ceulemans, *J. Am. Chem. Soc.* **1977**, *99*, 2208–2214; b) L. G. Vanquickienborne, A. Ceulem-

© 2009 Wiley-VCH Verlag GmbH & Co. KGaA, Weinheim

ans, *Inorg. Chem.* **1978**, *17*, 2730–2736; c) L. G. Vanquickienborne, A. Ceulemans, *Coord. Chem. Rev.* **1983**, *48*, 157–202; d) E. Larsen, G. N. La Mar, *J. Chem. Educ.* **1974**, *51*, 633–640; e) G. L. Miessler D. A. Tarr, *Inorganic Chemistry* 2nd ed. Prentice Hall Inc, New Jersey, **2000**.

[19] G. B. Porter, R. H. Sparks, *J. Photochem.* **1980**, *13*, 123–131.

[20] L. Yang, F. Okuda, K. Kobayashi, K. Nozaki, Y. Tanabe, Y. Ishii, M. Masa-aki Haga, *Inorg. Chem.* **2008**, *47*, 7154–7165.

[21] A. R. McDonald, M. Lutz, L. S. von Chrzanowski, G. P. M. van Klink, A. L. Spek, G. van Koten, *Inorg. Chem.* **2008**, *47*, 6681–6691.

[22] M. J. Frisch, G. W. Trucks, H. B. Schlegel, G. E. Scuseria, M. A. Robb, J. R. Cheeseman, J. A. Montgomery Jr, T. Vreven, K. N. Kudin, J. C. Burant, J. M. Millam, S. S. Iyengar, J. Tomasi, V. Barone, B. Mennucci, M. Cossi, G. Scalmani, N. Rega, G. A. Petersson, H. Nakatsuji, M. Hada, M. Ehara, K. Toyota, R. Fukuda, J. Hasegawa, M. Ishida, T. Nakajima, Y. Honda, O. Kitao, H. Nakai, M. Klene, X. Li, J. E. Knox, H. P. Hratchian, J. B. Cross, C. Adamo, J. Jaramillo, R. Gomperts, R. E. Stratmann, O. Yazyev, A. J. Austin, R. Cammi, C. Pomelli, J. W. Ochterski, P. Y. Ayala, K. Morokuma, G. A. Voth, P. Salvador, J. J. Dannenberg, V. G. Zakrzewski, S. Dapprich, A. D. Daniels, M. C. Strain, O. Farkas, D. K. Malick, A. D. Rabuck, K. Raghavachari, J. B. Foresman, J. V. Ortiz, Q. Cui, A. G. Baboul, S. Clifford, J. Cioslowski, B. B. Stefanov, G. Liu, A. Liashenko, P. Piskorz, I. Komaromi, R. L. Martin, D. J. Fox, T. Keith, M. A. Al-Laham, C. Y. Peng, A. Nanayakkara, M. Challacombe, P. M. W. Gill, B. Johnson, W. Chen, M. W. Wong, C. Gonzalez, J. A. Pople, *Gaussian 03*, Revision B.03, Gaussian, Inc., Pittsburgh, PA, **2003**.

Received: December 26, 2008

Published Online: March 31, 2009

© 2009 Wiley-VCH Verlag GmbH & Co. KGaA, Weinheim